Journal of Hazardous Materials 308 (2016) 37–49

Contents lists available at ScienceDirect

Journal of Hazardous Materials

journal homepage: www.elsevier.com/locate/jhazmat

Hazards of low dose flame-retardants (BDE-47 and BDE-32): Influence on transcriptome regulation and cell death in human liver cells

Quaiser Saquib[a,b,*], Maqsood A. Siddiqui[a,b], Javed Ahmed[a,b], Abdullah Al-Salim[a,b], Sabiha M. Ansari[c], Mohammad Faisal[c], Abdulaziz A. Al-Khedhairy[a], Javed Musarrat[d,e], Hend A. AlWathnani[c], Abdulrahman A. Alatar[c], Saud A. Al-Arifi[a]

[a] Zoology Department, College of Sciences, King Saud University, P.O. Box 2455, Riyadh 11451, Saudi Arabia
[b] A.R. Al-Jeraisy Chair for DNA Research, Zoology Department, College of Sciences, King Saud University, P.O. Box 2455, Riyadh 11451, Saudi Arabia
[c] Department of Botany & Microbiology, College of Sciences, King Saud University, P.O. Box 2455, Riyadh 11451, Saudi Arabia
[d] Department of Agricultural Microbiology, Faculty of Agricultural Sciences, Aligarh Muslim University, Aligarh 202002, India
[e] Baba Ghulam Shah Badshah University, Rajouri 185131, Jammu and Kashmir, India

HIGHLIGHTS

- First report on low dose molecular toxicity of BDE-47 and BDE-32.
- Both congeners induce DNA damage and mitochondrial dysfunction in HepG2 cells.
- Transcriptomic alterations were found in BDE-47 and BDE-32 treated cells.
- BDE-47 and BDE-32 exposure trigger apoptosis in HepG2 cells.

GRAPHICAL ABSTRACT

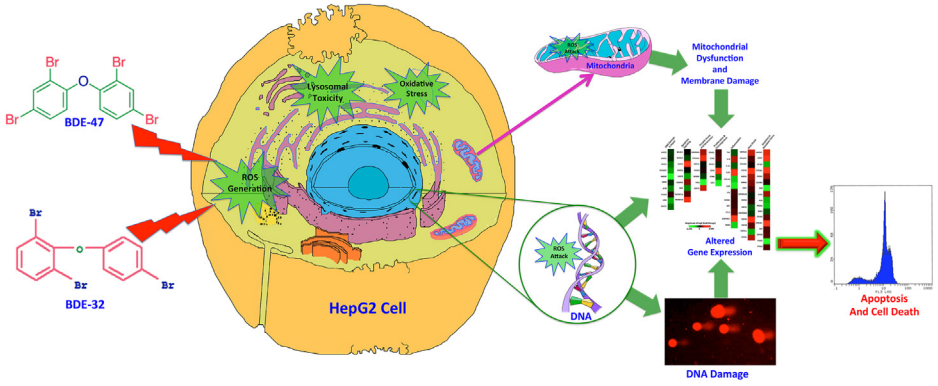

ARTICLE INFO

Article history:
Received 1 September 2015
Received in revised form
21 December 2015
Accepted 10 January 2016
Available online 13 January 2016

Keywords:
BDE-47
BDE-32
Flame-retardants
Cell death
Oxidative stress

ABSTRACT

We have evaluated the *in vitro* low dose hepatotoxic effects of two flame-retardants (BDE-47 and BDE-32) in HepG2 cells. Both congeners declined the viability of cells in MTT and NRU cell viability assays. Higher level of intracellular reactive oxygen species (ROS) and dysfunction of mitochondrial membrane potential ($\Delta\Psi m$) were observed in the treated cells. Comet assay data confirmed the DNA damaging potential of both congeners. BDE-47 exposure results in the appearance of subG_1 apoptotic peak (30.1%) at 100 nM, while BDE-32 arrested the cells in G_2/M phase. Among the set of 84 genes, BDE-47 induces downregulation of majority of mRNA transcripts, whilst BDE-32 showed differential expression of transcripts in HepG2. The ultrastructural analysis revealed mitochondrial swelling and degeneration of cristae in BDE-47 and BDE-32 treated cells. Overall our data demonstrated the hepatotoxic potential of both congeners *via* alteration of vital cellular pathways.

* Corresponding author at: Zoology Department, College of Sciences, King Saud University, P.O. Box 2455, Riyadh 11451, Saudi Arabia.
E-mail addresses: quaiser.saquib0@gmail.com, qsaquib@ksu.edu.sa (Q. Saquib).

http://dx.doi.org/10.1016/j.jhazmat.2016.01.025
0304-3894/

1. Introduction

Polybrominated diphenyl ethers (PBDEs) have been extensively used in the manufacturing of electrical appliances, textiles, carpets and furniture industries [1]. PBDEs are additive flame-retardants that are mixed into plastics, foam or sprayed onto fabrics. During the use and lifetime of the product, PBDEs exhibited their tendency to migrate from the material [2]. Such properties resulted in the ubiquitous presence of PBDEs in indoor dust and air. As a result, the possibility of their transfer into the wider environment to contaminate ecosystem and food chains is higher [3]. In addition, the bioaccumulative and persistence characteristics of PBDEs raised an increasing alarm over their potential adverse effects to human health [1,4]. Recent human biomonitoring studies revealed the presence of PBDEs in placenta and umbilical cord blood [5,6]. An increased level of PBDEs has been detected in human serum samples and correlated with altered hormone level in the exposed males [7].

BDE-47 is one of the prevalent congener found in both abiotic and biotic environments [8]. Neurodevelopmental changes have been attributed in children's exposed to BDE-47 *via* fetal cord blood [9]. Animal studies have revealed that BDE-47 had a toxic effect on liver, reproductive and central nervous systems [10–12]. *In vitro* exposure of A549, NCI-H358, Jurkat and mouse cerebellar granule neurons with BDE-47 exhibited significant decline in cell viability, mainly through overproduction of ROS and mitochondrial dysfunction [13–15]. HTR-8/SVneo cells treated with higher doses of BDE-47 (15 and 20 μM) stimulated the release of inflammatory cytokines (IL-6 and IL-8) [16]. Human neuroblastoma (SH-SY5Y) cells exposed to higher concentrations (1, 5 and 10 μmol/L) of BDE-47 showed cytotoxicity, apoptosis and upregulation of DAPK, caspase 3, 12 and cytochrome c mRNA transcripts, which indicates its neurotoxic potential [17]. At the similar concentrations (1, 5 and 10 μmol/L), BDE-47 activated the mitochondrial apoptotic pathway by upregulating p53, bax, cytochrome c and caspase 3 transcripts, with simultaneous down regulation of bcl-2 and bcl-2/bax ratio in SH-SY5Y cells [18]. At low doses, human neuroblastoma (SK-N-MC) cells co-exposed with BDE-47 and BDE-99 exhibited synergistic neurotoxic effects [19]. Interestingly, HepG2 cells treated with high doses of BDE-47 (6.25–100 μM) showed an involvement of lysosomes in mitochondrial-apoptotic pathway [20].

As yet, the available data on BDE-47 toxicity are mainly derived from studies at high doses and oriented towards its neurotoxic effects. The study of environmentally relevant doses has been the focus of National Institute of Environmental Health Sciences (NIEHS) [21]. For *in vitro* study, the exposure concentrations at nanomolar levels were recommended to investigate the toxic effects of BDE-47 at an environmentally relevant concentration [22]. In this relation, a single report on BDE-47 has demonstrated that low doses of BDE-47 (10^{-10}, 10^{-9} and 10^{-8} M) induces hormesis effects and activate DNA-PKcs/Akt pathway in HepG2 cells [23]. To the best of our knowledge, we did not encountered any study, which has attempted to demonstrate the hepatotoxic effect of PBDEs in nanomolar range, and to decipher cross talk between toxicity and oxidative stress pathways. Therefore, the purpose of this study is to test two PBDEs congeners (BDE-47 and BDE-32) for their hepatotoxic potential in HepG2 cells at different time periods, as well as to understand the activation of molecular pathways at environmentally realistic concentrations. It should be noted that, no study has been conducted so far on the toxicity of BDE-32. Therefore, we are unable to quote any literature for BDE-32. Hence, in this report, we assessed the effects of BDE-47 and BDE-32 on the (i) cell viability, (ii) intracellular ROS production and mitochondrial membrane potential ($\Delta\Psi m$), (iii) DNA strand breaks, (iv) cell cycle dysregulation, and (v) transcriptomics of a set of 84 human stress and toxicity pathway genes.

2. Materials and methods

2.1. Chemicals

2,2′,4,4′-Tetrabromodiphenyl ether (BDE-47, CAS No. 5436-43-1) (50 μg/mL in isooctane, 99.99% grade purity) and 2,4′,6-tribromodiphenyl ether (BDE-32, CAS No. 189084-60-4) (50 μg/mL in isooctane, 99.99% grade purity) were purchased from AccuStandard, Inc., USA. Dimethyl sulfoxide (DMSO) for molecular biology (99.9%) (Cat. No. D8418), propiodium iodide (≥94%) (Cat. No. P4170), Na_2-EDTA (99.9%) (Cat. No. E5134), Tris [hydroxymethyl] aminomethane (99.9%) (Cat. No. 93362), RNAseA from bovine pancreas (90 U/mg) (Cat. No. 83831), 2′,7′-dichlorofluorescin diacetate (DCFH-DA) (≥97%) (Cat. No. D6883), rhodamine 123 (Rh123) (≥85%) (Cat. No. 83702), normal melting agarose (NMA) (Cat. No. A6013, type I), low melting agarose (LMA) (Cat. No. A9414, low gelling temperature), ethyl methanesulfonate (EMS) (Cat. No. M0880) and neutral red (≥90%) (Cat. No. N7005), thiazolyl blue tetrazolium bromide (MTT) (≥97%) (Cat. No. M5655), Dulbecco's modified eagle's medium-high glucose (DMEM) (Cat. No. D5648), Dulbecco's phosphate buffered saline (PBS, Ca^{2+}, Mg^{2+} free) (Cat. No. D5652) were purchased from Sigma Chemical Company, St. Louis, MO, USA. Antibiotic-antimycotic solution (100X) (Cat. No. 15240-062), fetal bovine serum (FBS) (Cat. No. 26140-079) was procured from ThermoFisher Scientific, USA. All other chemicals were of analytical grade unless otherwise stated. Culture wares and other plastic consumables used in the study were procured commercially from Nunc, Denmark.

2.2. Cell culture and BDE-47, BDE-32 exposure

Human liver hepatocellular carcinoma (HepG2) cells were purchased from ATCC, USA. Cells were cultured in DMEM supplemented with 10% fetal bovine serum (FBS), antibiotic-antimycotic solution (100X, 1 mL/100 mL of medium), and incubated at 37 °C in a humidified atmosphere containing 5% CO_2. Each batch of cells was assessed for cell viability by trypan blue dye exclusion test and batches showing more than 95% cell viability were used for experiments. For BDE exposure, cells were first seeded in 96-well plates at a concentration of 1×10^4/100 μL/well and left to attach for 24 h. Ensuring the confluency of cells, the culture media were discarded, and fresh medium containing various concentrations (25, 50 and 100 nM) of BDE-47 and BDE-32 were added to the cells and allowed to grow for 3 and 6 days.

2.3. Thiazolyl blue tetrazolium bromide (MTT) assay

The MTT is a water-soluble, positively charged dye, which becomes water-insoluble by the mitochondrial dehydrogenase system, and actively penetrates the viable cells [24]. BDE-47 and BDE-32 induced decline in cell viability was determined by MTT assay following our previously described method [25]. In brief, cells (1×10^4) were exposed to BDE-47 and BDE-32 in the concentration range of 25, 50 and 100 nM for 3 and 6 days. After the exposure time, MTT (5 mg/mL stock in PBS) was added in the volume of 10 μL/well in 100 μL of cell suspension, and the plate was incubated for 4 h at 37 °C. At the end of incubation period, aqueous medium was carefully aspirated and 200 μL of DMSO was added in each well and mixed gently. Microplate was then kept on a rocker shaker for 10 min at room temperature and the purple color was read on a microplate reader at 550 nm (Multiskan Ex, Thermo Scientific, Finland). Untreated controls were also run under identical conditions.

2.4. Neutral red uptake (NRU) cell viability assay

The NRU assay relies on a weak cationic supravital dye, known to actively penetrate the membranes of live cells by nonionic passive diffusion and concentrates in the lysosomes [26]. Reduction in the viability of HepG2 cells was determined by NRU assay following our previously described procedure [25]. Briefly, cells were exposed to BDE-47 and BDE-32 in the concentration range of 25, 50 and 100 nM for 3 and 6 days. After the exposure time, medium was aspirated and cells were washed twice with PBS, and incubated for 3 h in a medium supplemented with neutral red (50 μg/mL). Medium was washed off rapidly with a solution containing 0.5% formaldehyde and 1% calcium chloride. Cells were subjected to further incubation of 20 min at 37 °C in a mixture of acetic acid (1%) and ethanol (50%) to extract the dye and the absorbance was read at 540 nm on a microplate reader. The values were compared with control set run under identical conditions.

2.5. Flow cytometric analysis of ROS and $\Delta\Psi$m

Intracellular ROS generation was determined using a fluorescent probe DCFH-DA [27]. However, $\Delta\Psi m$ was determined by observing changes in the fluorescence intensity of mitochondrial-specific cationic dye Rh123 [28]. In brief, cells treated with varying concentrations (25, 50 and 100 nM) of BDE-47 and BDE-32 for 3 and 6 days were trypsinized and spin down at 3000 rpm for 5 min. The pellets were aliquoted in two tubes and washed twice with cold PBS, followed by the addition of PBS (500 μL) containing DCFH-DA (5 μM) and PBS (500 μL) containing Rh123 (5 μg/mL) in aliquoted tubes. All samples were incubated for 60 min at 37 °C in dark. Cells were again washed twice with PBS and finally suspended with 500 μL of PBS. The fluorescence of 10,000 cells were recorded upon excitation at 488 nm at FL1 Log channel through 525 nm band-pass filter on Beckman Coulter flow cytometer (Coulter Epics XL/Xl-MCL, USA).

2.6. Transmission electron microscopy (TEM) of HepG2 cells

BDE-47 and BDE-32 induced changes in mitochondrial structure was analyzed using TEM following our previously described method [29]. In brief, cell pellets from control, BDE-47 and BDE-32 (100 nM, 6 days) were fixed in glutaraldehyde for 10 min, followed by re-suspension of cells in OsO_4 (1%) for 1 h at 4 °C. An additional incubation of 1 h were given for each cell suspension in 2% aqueous uranyl acetate solution pursued by the dehydration of cells using ascending grade of ethanol. Cells were finally embedded in low viscosity araldite resin and ultrathin sections of 80 nm were made for TEM analysis under high vacuum (100 kV).

2.7. DNA damage analysis by comet assay

Comet assay was performed following the method described previously by Saquib et al. [30]. HepG2 cells exposed for 3 days with 25, 50 and 100 nM of BDE-47 and BDE-32 were detached and centrifuged at 3000 rpm for 3 min. The cells (4×10^4) from untreated and treated groups were suspended in 100 μL of Ca^{2+} Mg^{2+} free PBS and mixed with 100 μL of 1% low melting agarose (LMA). The cell suspension (80 μL) was then layered on one-third frosted slides, pre-coated with normal melting agarose (NMA) (1%) and kept at 4 °C for 10 min. After gelling, 90 μL of LMA (0.5% in PBS) was added and left for solidifying on ice pack. The cells were lysed in a lysing solution for overnight and subjected to electrophoresis at 0.7 V/cm for 30 min (300 mA, 24 V) at 4 °C followed by washing of slides with neutralization buffer. All preparative steps were conducted in dark to prevent secondary DNA damage. The slides were stained with 75 μL of ethidium bromide (20 μg/mL) for 5 min and the comet images were analyzed at 40× magnification using a fluorescence microscope (Nikon Eclipse 80i, Japan) coupled with charge coupled device (CCD) camera. Images from 50 cells (25 from each replicate slide) were randomly selected and subjected to image analysis using Comet Assay IV software (Perceptive Instruments, Suffolk, UK). The data were subjected to one-way analysis of variance (ANOVA). Mean values of the tail length (μm), Olive tail moment (OTM) and tail intensity (%) were separately analyzed for statistical significance.

2.8. Cell cycle analysis

HepG2 cells treated with varying concentrations (25, 50 and 100 nM) of BDE-47 and BDE-32 for 3 and 6 days were trypsinized and processed for cell cycle analysis following our previously described method [25]. In brief, the harvested cells were centrifuged at 3000 rpm for 5 min and pellets were fixed with 500 μL of chilled 70% ethanol, and incubated at 4 °C for 1 h. After two successive washes, cell pellets were again suspended in 500 μL PBS containing propiodium iodide (50 μg/mL), 0.1% Triton X-100 and 0.5 mg/mL RNAase A. The cells were left for staining for 1 h at 37 °C in dark. The red fluorescence of 10,000 events of propiodium iodide stained cells were acquired at a laser excitation of 488 nm, and 620 nm band-pass filter using Beckman Coulter flow cytometer. The data were analyzed by excluding the cell debris, characterized by a low FSC/SSC, using Beckman Coulter flow cytometer (Coulter Epics XL/Xl-MCL, USA and System II Software, Version 3.0).

2.9. Isolation of total RNA and RT^2 profiler PCR array

PCR array experiments were done following our previously described method [25]. In brief, total RNA was isolated separately from 3×10^5 cells/well from control, and cells exposed to 100 nM of BDE-47 and BDE-32 for 6 days using the commercially available kit (RNeasy Mini Kit, Cat. No. 74106, Qiagen, USA). RNA purification was done using the iPrep™ PureLink™ kit (Invitrogen, USA) by Invitrogen® automated system following the manufacturer's protocol. Purity of total RNA was verified by the use of a Nanodrop 8000 spectrophotometer (Thermo Scientific, USA) and the integrity of RNA was visualized on 1% agarose gel using gel documentation system (Universal Hood II, BioRad, USA). The first-strand cDNA synthesis was performed with 1 μg of total RNA and 100 ng of oligo-p(dT) 12-18 primer and MLV reverse transcriptase (GE Health Care, UK) according to the manufacturer's recommendations. Changes in the relative gene expression of 84 genes responsible for human stress and toxicity pathway were quantified using RT^2 Profiler™ PCR Array (Cat. No. PAHS-003 A, SABiosciences Corporation, Frederick, MD) in a 96-well array format. cDNA equivalent to 1 μg of total RNA was used for each array. The arrays were run on Roche® LightCycler® 480 (96-well block) (IN, USA) following the recommended cycling programs. Expression data obtained with BDE-47 and BDE-32 treatments were normalized to the average $^{\Delta}$Ct value of five housekeeping genes (*B2M*, *HPRT1*, *RPL13A*, *GAPDH* and *ACTB*) and expressed with respect to the untreated control. RT-PCR array data were evaluated from at least three independent experiments and the resultant $^{\Delta}C_t$ values were combined to calculate the average fold regulation values. Genes that were significantly different for BDE-47 and BDE-32 *versus* control were determined by Students *t*-test ($p < 0.05$) by comparing the $^{\Delta}$Ct values for the triplicate trials for each test sample with the $^{\Delta}$Ct values for the control.

2.10. Statistical analysis

Data were expressed as mean ± S.D. for the values obtained from at least three independent experiments done in triplicate. Statistical analysis was performed by one-way analysis of variance (ANOVA) followed by Dunnett's multiple comparisons test

(Sigma Plot 11.0, USA). The level of statistical significance chosen was $p < 0.05$, unless otherwise stated.

3. Results

3.1. Assessment of cell viability by MTT and NRU assays

HepG2 cells treated with 25, 50 and 100 nM of BDE-47 for 3 and 6 days exhibited significant reduction of 14.3%, 15.4%, 15.4% and 11.6%, 26.7%, 28.6% cell viability in MTT assay (Fig. 1A). BDE-32 at the exposure concentrations of 25, 50 and 100 nM also showed 10.8%, 15.5%, 36.2% and 18.4%, 21.3%, 42.3% decline in the cell viability after 3 and 6 days of incubation (Fig. 1B). In NRU assay, both congeners exhibited a concentration and time dependent reduction in cell viability. After 3 and 6 days of incubation, BDE-47 at 25, 50 and 100 nM showed 0.8%, 7%, 10.5% and 39.5%, 50.6%, 55.8% decline in the viability of cells (Fig. 1C). BDE-32 after 3 and 6 days of incubation induces 7.4%, 15%, 42% and 19.2%, 38.3%, 45.11% decline in cell viability at 25, 50 and 100 nM treatment concentrations (Fig. 1D). The morphological analysis of BDE-47 and BDE-32 treated cells explicitly demonstrated the toxicity, manifested as detachment of the adherent cells at increasing concentrations of both congeners (Fig. 1 in Supplementary data).

3.2. Intracellular ROS generation

Flow cytometric analysis revealed an increase in the intracellular ROS formation by BDE-47 and BDE-32. Compared to 100% DCF fluorescence in control, HepG2 cells treated with 50 and 100 nM of BDE-47 for 3 days showed significant 111% and 114% increase in ROS generation. BDE-47 exposure for 6 days enhanced the ROS formation at all concentrations (25, 50 and 100 nM) by 111%, 117% and 114% (Fig. 2A). Likewise, ROS level was also elevated in cells treated with varying concentrations of BDE-32 for 3 and 6 days. Comparative to 100% fluorescence in control, BDE-32 (25, 50 and 100 nM) exposure for 3 and 6 days exhibited 114%, 116%, 115% and 121%, 127, 130% higher ROS generation in cells (Fig. 2B).

3.3. Effect of BDE-47, BDE-32 on $\Delta\Psi$m and mitochondrial structure

Our flow data showed a differential change in the $\Delta\Psi m$ of cells exposed to BDE-47. After 3 days, BDE-47 at the concentrations of 50 and 100 nM exhibited 11% and 12.4% decline in $\Delta\Psi m$. However, after 6 days, the $\Delta\Psi m$ were found increased by 39%, 43% and 42% at 25, 50 and 100 nM (Fig. 2C). On the other hand, BDE-32 exhibited a concentration and time depend decline in $\Delta\Psi m$. Cells treated with 25, 50 and 100 nM of BDE-32 for 3 and 6 days showed 7%, 10%, 13% and 18%, 20%, 27% decline in $\Delta\Psi m$, as compared to control (Fig. 2D). Considering the differences in fluorescence pattern of Rh123, we further analyzed the structural changes in mitochondria. Within the control cell, a bean-shaped mitochondria with a highly folded inner membrane, exhibiting conspicuous cristae was observed (Fig. 3A and B). In comparison, the BDE-47 treated cells showed swollen mitochondria with degenerated cristae (Fig. 3C and D). On the other hand, BDE-32 treated cells exhibited partial degeneration of cristae. However, BDE-32 treatment did not resulted in the swelling of mitochondria (Fig. 3E and F).

3.4. Effect of BDE-47 and BDE-32 on DNA

The representative comet images demonstrate the extent of broken DNA liberated from the comet heads at increasing concentrations of both congeners (Fig. 4I and II). After 3 days, BDE-47 at the highest concentration of 100 nM showed 6-fold higher OTM value ($p < 0.01$), as compared to control OTM (0.44 ± 0.05) (Table 1).

Table 1
BDE-47 and BDE-32 induced DNA damage in HepG2 cells after 3 days of exposure, analyzed using different parameters of alkaline comet assay.

Groups	Olive tail moment (arbitrary unit)	Tail length(μm)	Tail intensity (%)
Control	0.44 ± 0.05	43.71 ± 2.11	3.95 ± 0.15
EMS (2 mM)	$8.23 \pm 1.33^{**}$	$98.56 \pm 4.38^{**}$	$12.36 \pm 1.12^{**}$
BDE-47 (nM)			
25	$0.99 \pm 0.07^{**}$	$50.29 \pm 0.98^{**}$	$5.92 \pm 0.22^{**}$
50	$1.75 \pm 0.12^{**}$	$57.51 \pm 1.13^{**}$	$8.05 \pm 0.17^{**}$
100	$2.64 \pm 0.10^{**}$	$59.20 \pm 1.06^{**}$	$11.26 \pm 0.30^{**}$
Control	0.38 ± 0.06	42.40 ± 1.75	3.17 ± 0.24
EMS (2 mM)	$7.93 \pm 0.69^{**}$	$88.26 \pm 3.88^{**}$	$18.45 \pm 1.8^{**}$
BDE-32 (nM)			
25	$1.48 \pm 0.24^{**}$	$51.09 \pm 0.19^{*}$	$9.40 \pm 0.68^{**}$
50	$1.70 \pm 0.38^{**}$	$55.41 \pm 1.95^{**}$	$9.60 \pm 0.70^{**}$
100	$2.41 \pm 0.26^{**}$	$55.70 \pm 5.51^{**}$	$12.60 \pm 0.74^{**}$

Data represent the mean ± S.D. of three independent experiments done in duplicate. EMS: ethyl methanesulphonate.
* $p < 0.05$.
** $p < 0.01$.

Relative to control OTM (0.38 ± 0.06), BDE-32 at the highest concentration of 100 nM exhibited 6.3-fold greater OTM value ($p < 0.01$) (Table 1). Nevertheless, the differences in distribution of DNA damage exist in the cell population. Variation in distribution of DNA damage by BDE-47 and BDE-32 exposure is shown in Fig. 4III and IV.

3.5. Dysregulation of cell cycle

The representative cell cycle images of HepG2 cells revealed that BDE-47 treatment for 3 days arrests the cells in G_2/M phase. After 6 days, the treated cells showed a gradual decline in G_2/M peak with subsequent appearance of subG$_1$ apoptotic peak at increasing concentrations (Fig. 5I). On the other hand, BDE-32 exposure resulted in G_2/M arrest in HepG2 cells both after 3 and 6 days of exposure (Fig. 5I). An average data analysis of cell cycle revealed that BDE-47 (50 and 100 nM) exposure for 3 days induced significant $27.5 \pm 1.7\%$ and $25.9 \pm 0.9\%$ ($p < 0.01$ and $p < 0.05$) increase in G_2/M peak (Fig. 5II, A). Subsequent incubation for 6 days resulted in the appearance of $17.9 \pm 1.8\%$ and $30.1 \pm 1.0\%$ ($p < 0.05$ and $p < 0.01$) of subG$_1$ peak (Fig. 5II, B). After 3 days, BDE-32 (50 and 100 nM) treatment showed $30.3 \pm 0.6\%$ and $32.5 \pm 1.7\%$ cells in G_2/M phase. Moreover, 6 days of treatment resulted in the increase in G_2/M peak to $45.1 \pm 3.3\%$ and $47.4 \pm 1.8\%$, respectively (Fig. 5II, C and D). No increase in apoptotic peak was observed after 6 days of exposure with BDE-32.

3.6. BDE-47 and BDE-32 induced transcriptomic alterations

BDE-47 (100 nM) treated cells induce downregulation of majority of genes related to seven different pathways. Within the DNA damage and repair pathway, *RAD50* and *ERCC1* genes exhibited maximal downregulation of 2.2 and 3.1-folds. In apoptosis signaling pathway, *CASP8*, *TNFRSF1A* and *NFKBIA* genes were upregulated to 1.2, 3.4 and 3.3-folds. Out of 17 genes in oxidative or metabolic stress pathway, *HMOX1*, *SOD2*, *PRDX1* and *PTGS1* genes showed upregulation of 3.3, 3.1, 1.1 and 1.0-folds. Within the same pathway, *CYP1A1* and *CYP2E1* genes were downregulated to 2.9 and 1.8-folds. Among the inflammatory pathway, *IL-6*, *IL1b*, *TNF* and *NFKB1* genes were downregulated to 3.0, 3.1, 1.1 and 1.0-folds, respectively (Fig. 6A).

HepG2 cells treated with BDE-32 (100 nM) for 6 days exhibited differential expression of genes. The corresponding heat map suggested strong oxidative or metabolic stress, growth arrest and senescence, activation of pro-inflammatory and heat shock

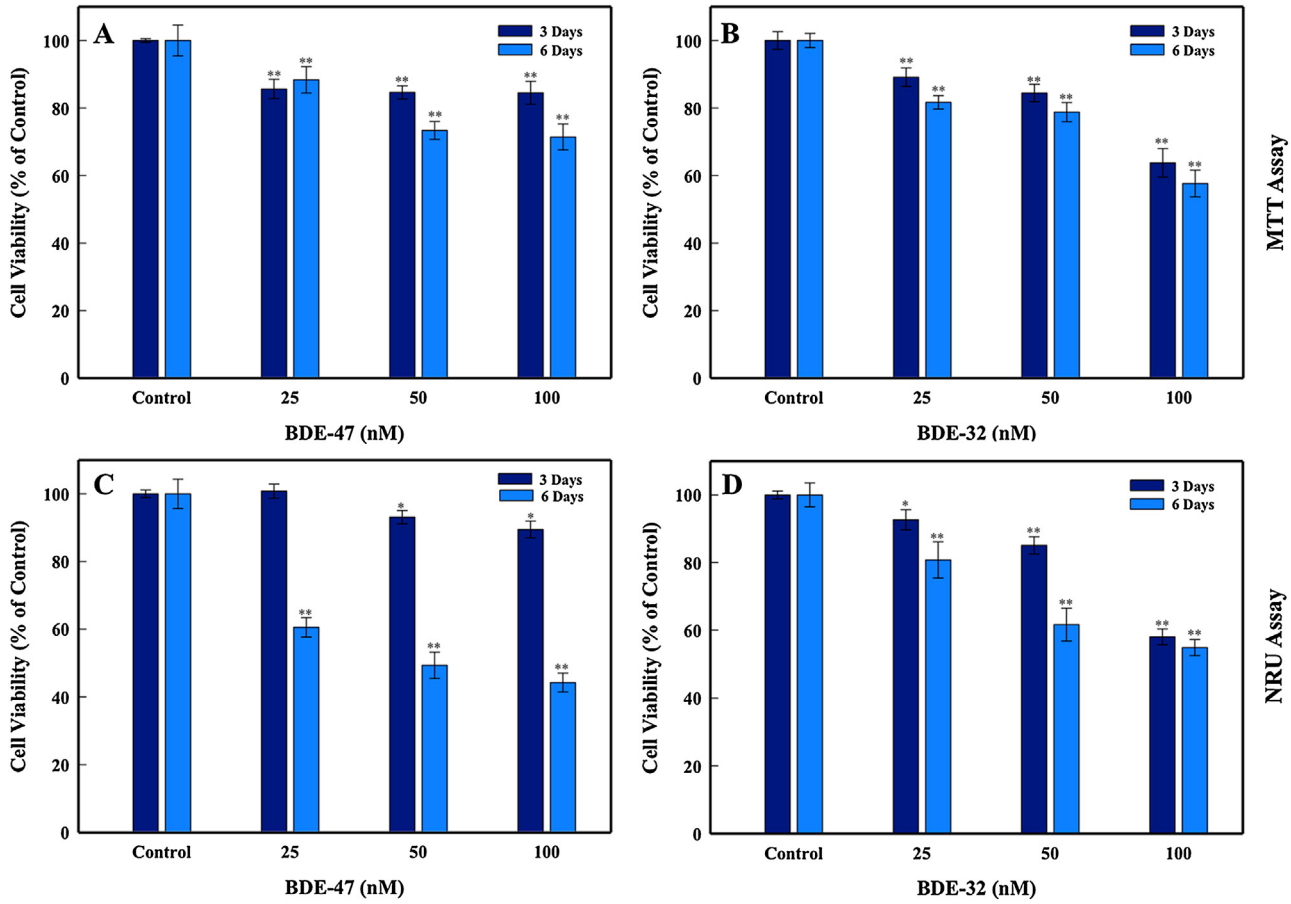

Fig. 1. BDE-47 (A) and BDE-32 (B) induced reduction in cell viability analyzed by MTT assay. NRU assay showing BDE-47 (C) and BDE-32 (D) induced decline in HepG2 viability. $^{*}p < 0.05$, $^{**}p < 0.01$ *versus* control.

responses upon BDE-32 treatment. Among 19 genes for oxidative or metabolic stress, *CYP1A1* has exhibited a maximum of 11.3-fold upregulation. Also, *CYP2E1*, *SOD2* and *HMOX1* genes were upregulated by 5.2, 4.6 and 2.8-folds. Within the set of 7 genes responsible for growth arrest and senescence, *GADD45A*, *CDKN1A*, *DDIT3*, *MDM2* genes have exhibited 1.9, 3.4, 2.3 and 1.1-folds upregulation. A maximum downregulation of 4.8-folds has been observed for *TP53* gene. Out of 12 pro-inflammatory genes, *IL-6*, *IL1b*, *SERPINE1* were maximally upregulated to 2.0, 4.5 and 7.4-folds. *EGR1*, *CCNC* and *CCND1* genes in proliferation and carcinogenesis were upregulated to 10.4, 1.3 and 1.2-folds. *RAD50* and *UNG* were maximally down regulated to 6.6 and 2.2-folds in DNA damage and repair pathway. Within the apoptosis signaling pathway, *CASP1*, *CASP10*, *TNFRSF1A* and *TNFRSF10* were upregulated to 7.5, 1.6, 3.3 and 4.0-folds, respectively (Fig. 6B).

4. Discussion

Due to the wider application of flame-retardants in household and commercial products human exposure to PBDEs increased exponentially over recent decades [31]. Based on the analysis of 2062 human serum samples in 2003-2004, BDE-47 was detected in nearly all participants and ranked top among the measured PBDE congeners [32]. Despite these facts, the hepatotoxic effects of BDE-47 and the underlying mechanisms of toxicity are not well studied. The MTT assay indicated that both BDE-47 and BDE-32 significantly decreased the cell viability in a dose and time-dependent manner. Comparative to BDE-47, BDE-32 exposure for 6 days induce 1.2-folds higher reduction in cell viability. Our MTT data is in accordance with a recent report, which has demonstrated 29% and 53% loss of HepG2 cell viability after 24 h of treatment with BDE-47. However, the authors used much higher doses (50 and 100 μM) of BDE-47 [20], as compared to the nM concentrations used in the current study. Also, SH-SY5Y cells treated for 24 h with 4 and 8 μg/mL of BDE-47 exhibited significant decline of cell viability in MTT test [33]. In NRU assay, we found that BDE-47 and BDE-32, both induced a concentration and time-dependent loss of cell viability. Contrary to MTT assay results, BDE-47 showed more pronounced effect than BDE-32, which could be attributed to a greater lysosomal damage, as compared to the mitochondrial toxicity in MTT assay. Therefore, BDE-47-induced alterations in sensitive lysosomal membrane may lead to lysosomal fragility, which resulted in decreased uptake and binding of neutral red dye, possibly *via* decreasing the activity of lysosomal acid phosphatase in the cells [20]. Lysosomal destabilization is also regarded as a prior event of mitochondrial injury [34].

In order to confirm the mitochondrial dysfunction, flow cytometric analyses were done with both congeners. Our $\Delta\Psi m$ data on biphasic fluorescence pattern of Rh123 in BDE-47 and BDE-32 treated cells is quite intriguing. We found that HepG2 cells treated with BDE-47 for 3 days exhibited a declining pattern of Rh123 fluorescence, which gradually increased after 6 days of incubation. On the other hand, BDE-32 exposure resulted in decline of Rh123 fluorescence in a concentration and time-dependent manner. Rh123 due to the less lipophilic nature slightly perturbs the surface potential of membrane, and has similar kinetic constants for influx and efflux from mitochondrial matrix. As a result, Rh123 is a good candidate to measure the actual mitochondrial membrane potential

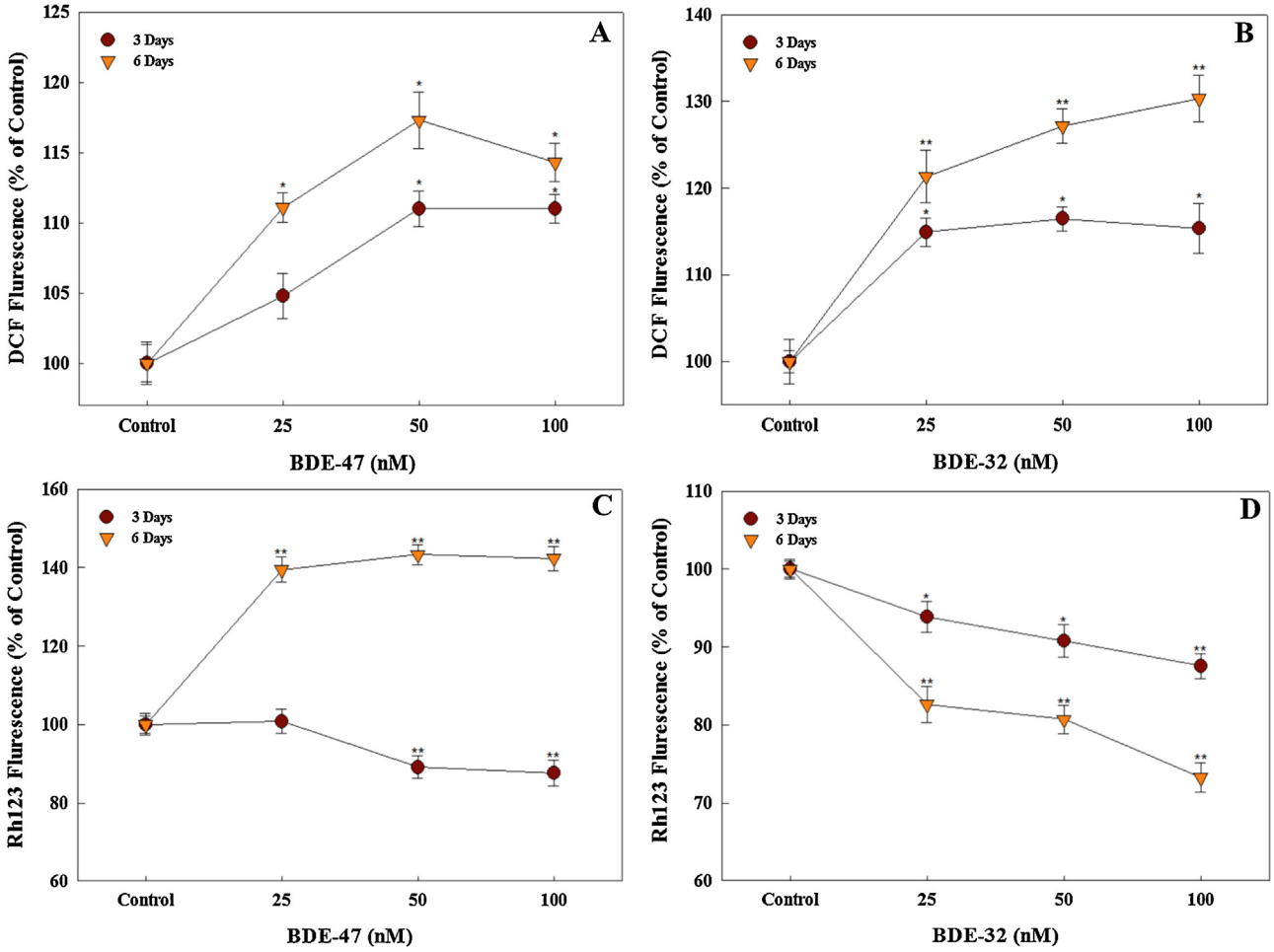

Fig. 2. Flow cytometric analysis of BDE-47 (A) and BDE-32 (B) induced ROS generation in HepG2 cells. Effect of BDE-47 (C) and BDE-32 (D) treatments on mitochondrial dysfunction of HepG2 cells. $^{*}p < 0.05$, $^{**}p < 0.01$ *versus* control.

[35]. A possible reason for fluorescence decline of Rh123 by BDE-47 (3 days) and BDE-32 (3 and 6 days) treatments could be due to the dissipation of $\Delta\Psi m$ by disruption of proton-moving force or the inner membrane permeability [25]. Our membrane potential data is in agreement with previous findings suggested the loss of $\Delta\Psi m$ by BDE-47 in human fetal liver hematopoietic stem, Jurkat and HepG2 cells [36,14,20].

However, an enhanced fluorescence of Rh123 in BDE-47 (6 days) treatment can be related with the mitochondrial property to swell under overwhelming conditions *viz.* Ca^{++} influx, pH and cytochrome c release during apoptotic cell death. It is reported that continuous opening of the pore in inner mitochondrial membrane (IMM) referred to as the mitochondrial permeability transition pore (MPPT), is followed by a release of Ca^{++} from the mitochondrial matrix along with termination of oxidative phosphorylation. These events initiate swelling of mitochondrial matrix by unfolding the inner membrane before the rupture of outer mitochondrial membrane [37]. When MPPT occurs, the associated channel opens, protons and ions equilibrate freely across the inner membrane, and osmotic disequilibrium ensues, which ultimately results in the swelling of matrix space [38]. In our TEM data, we also found mitochondrial swelling with degenerated inner membrane or cristae in BDE-47 treated cells, which supports this mechanism, and validate the fact that the altered mitochondria can no longer retain Rh123, as a result it leaks out from the mitochondrial membrane to the cytoplasm. This relocalization from the mitochondria to cytosol is an index of mitochondrial impairment with the disruption of mitochondrial membrane [39]. Our observation is in line with variation in mitochondrial morphology, indicating mitochondrial swelling in HepG2 cells treated with vitamin B12 analog hydroxycobalamin[c-lactam] [40]. On the other hand, the TEM analysis on BDE-32 treated cells showed partial degeneration of inner mitochondrial membrane or cristae. However, no size variation has been found in the mitochondria. These observations, substantially justify our above hypothesis of fluorescence decline in Rh123, owing to disturbance of $\Delta\Psi m$ in mitochondrial inner membrane. Overall, the ultrastructural analysis of mitochondria led us to conclude that HepG2 mitochondria reacts differently to both congeners. Nonetheless, future studies are warranted to reveal BDE-isomers specific responses in mitochondrial structure and its related toxicity. As a mitochondrial defect, the loss of $\Delta\Psi m$ has been strongly correlated with enhanced ROS generation in cells [41]. Thus, we further analyzed the ROS generation in HepG2 cells. Earlier studies have reported that high concentrations of BDE-47 could enhance the production of ROS [17,14]. Compared to the untreated control, BDE-47 and BDE-32 both showed significant overproduction of ROS in a dose and time-dependent manner. These data are in agreement with a single study on BDE-47 demonstrating ROS production in HepG2 at nM range [20]. Although, BDE-47 at μM concentrations has already been reported to produce ROS in HTR-8/SVneo, Jurkat and SH-SY5Y cells [16,14,19]. Therefore, our data unequivocally suggests the role of ROS in mitochondrial dysfunction.

It is commonly accepted that DNA is the potential target of ROS attack. Our comet data demonstrates that both congeners induce

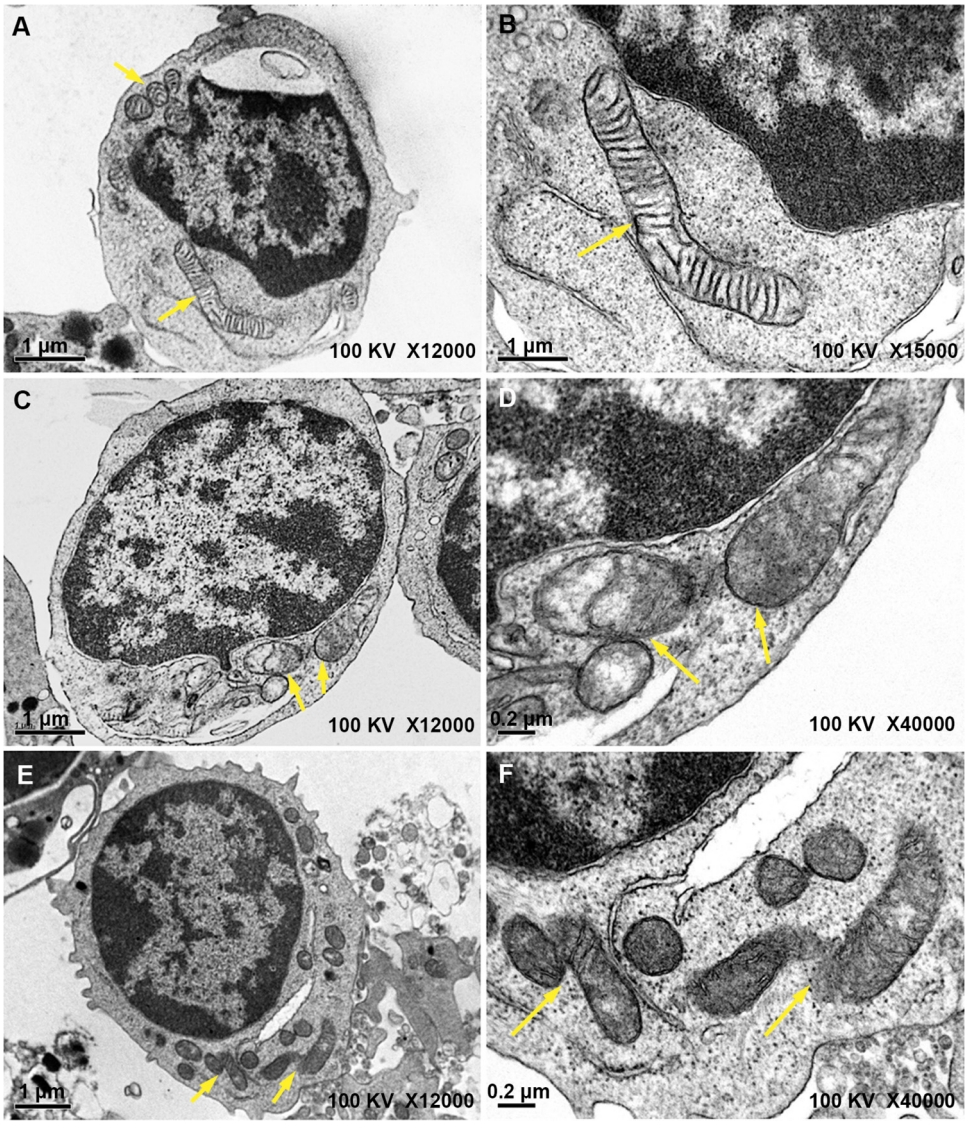

Fig. 3. Ultrastructural analysis of HepG2 cells treated with BDE-47 and BDE-32. (A) HepG2 cell in DMEM medium alone (control) showing the normal mitochondrial morphology. (B) Is the magnified view of the panel A mitochondria showing intact cristae. The BDE-47 (100 nM, 6 days) treated HepG2 cell in panel C showing swollen mitochondria. Panel D is the magnified image of panel C mitochondria with denigrated cristae. BDE-32 treated HepG2 cell showing partial degeneration of cristae (panel E). Panel F is the magnified view of mitochondria in panel E, no swelling has been observed in BDE-32 treatment. Arrows indicate mitochondria with damaged cristae.

significant DNA damage at nM concentrations. Compared to control, BDE-47 and BDE-32 at 100 nM showed 6 and 6.3-folds ($p < 0.01$) higher OTM values. In fact, BDE-32 induced more pronounced DNA damage than BDE-47 in HepG2 cells. Wang et al. [23] found no DNA damage in HepG2 cells after 24 h exposure with low doses (10^{-10}, 10^{-9} and 10^{-8} M) of BDE-47. Contrary to these observations, we found that HepG2 cells treated with 25, 50 and 100 nM ($p < 0.01$) of BDE-47 for 3 days showed significant level of DNA damage. Therefore, these observations reaffirm the possibility that cellular DNA repair machinery may have been adversely affected with extended exposure of both congeners. Consequently, the unrepaired DNA damage was detected in comet assay under alkaline conditions. Nonetheless, our comet data is substantiated by earlier report suggesting the DNA damaging properties of BDE-47 in human neuroblastoma cells [33].

Aberrant cell proliferation and DNA damage are usually associated with abnormal progression of cell cycle [23]. Our cell cycle data revealed that both congeners, after 3 days of treatment arrested the cells in G_2/M phase. However, BDE-47 exposure for 6 days showed an increase in the subG_1 apoptotic peaks, while BDE-32 increased the G_2/M peak in treated cells. It is known that cellular DNA repair mechanisms are highly conserved and extensive DNA damage may lead to cell cycle arrest and cell death [42–44]. Most likely, in case of 3 days treatment with BDE-47, the DNA damage induced at lower concentrations were not repaired during the G_2/M phase, consequently, the cells become apoptotic after 6 days. However, for BDE-32, an increase in G_2/M peak suggests that the cellular repair machinery were active to rectify the damage and prevent the cells to become apoptotic. Further investigations are necessary to draw firm conclusions to verify the exact pathways of such responses in BDE-32 exposed HepG2 cells. Our cell cycle data on BDE-47 is corroborated well with earlier reports suggesting BDE-47 induced apoptosis in cells [33,36].

Under the toxic conditions, damaged cells have the potential to amend the expression of genes to deregulate signalling pathways or reinstate checkpoint pathways [45]. In this relation, we analyzed an array of 84 genes related to toxicity and stress pathways. On a global scale, BDE-47 induce downregulation of genes, whereas BDE-32 resulted in the differential expression of mRNA transcripts, which suggest a distinct metabolic processing of both congeners by

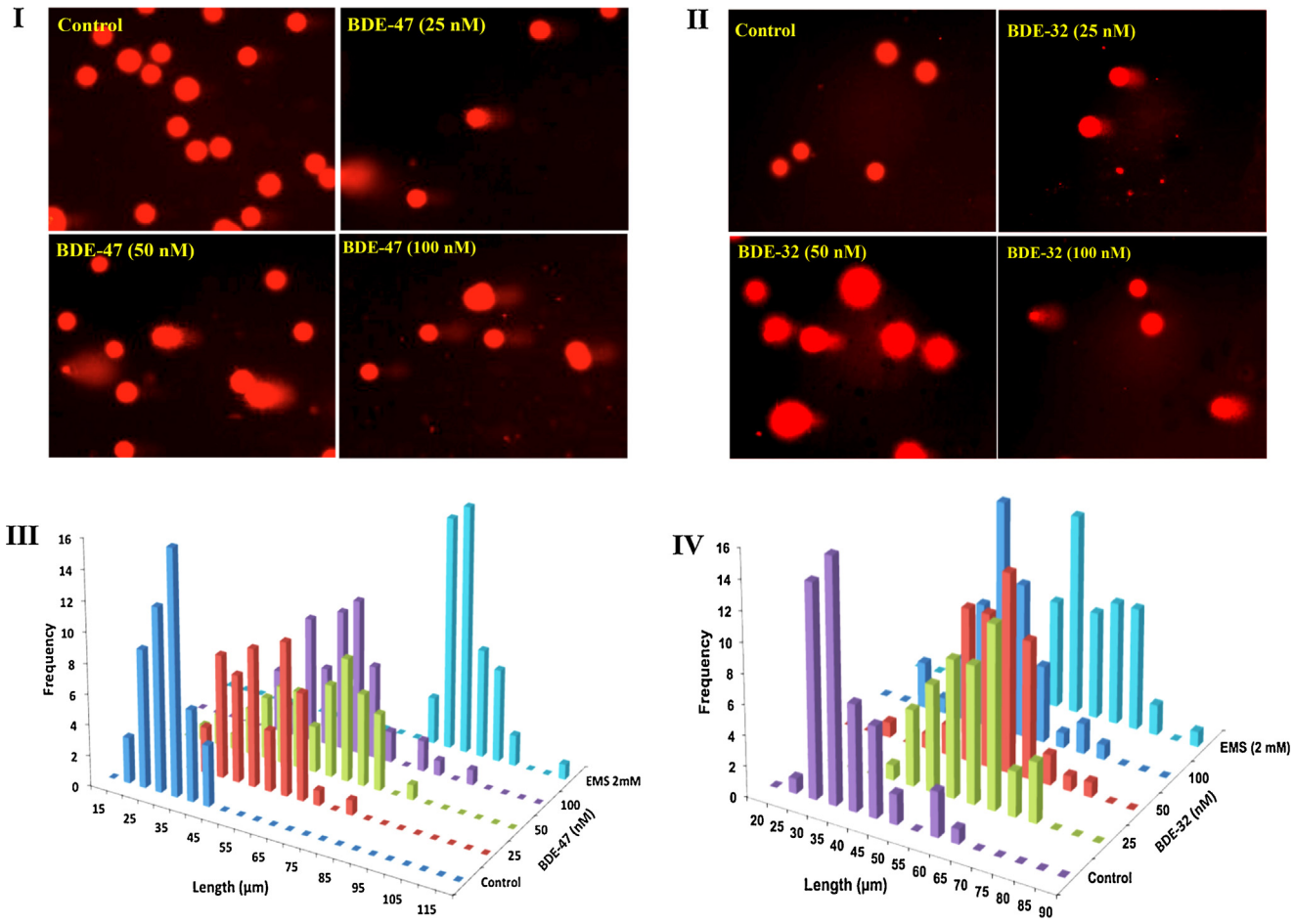

Fig. 4. Representative comet images showing DNA damage by BDE-47 (panel I) and BDE-32 (panel II) in HepG2 cells. Panel III and IV showing the frequency distribution of varying level of damaged DNA in terms of tail length (μm).

HepG2 cells. Nonetheless, BDE-47 and BDE-32 showed a common behavior by downregulating nearly all genes in the DNA damage and repair pathway, with maximal downregulation noticed for *ERCC1*, *RAD50* and *ATM* genes. *ERCC1* is one of the key players among 16 proteins responsible for nucleotide excision repair during DNA double-strand breaks [46]. In addition, another important gene responsible for base excision repair of DNA is *RAD50*, which form MRN complex (*MRE11*/*RAD50*/*NBS1*) to identify and bind the damaged DNA, unwind them and subsequently recruit and activate *ATM* [47]. The activated *ATM* further phosphorylates several key proteins including *p53*, which leads to cell cycle arrest, DNA repair or apoptosis [48]. The under expression of above genes unequivocally suggest that the DNA repair capacity of cells to rectify strand breaks has been severely affected [49]. Altogether, the PCR array data on the under expression of BDE-47 genes suggest a pleiotropic effect in HepG2 cells. Our data is in agreement with previous report suggesting the downregulation of array of genes related to different pathways in human leukaemia K562 cells treated with Myristicin [50].

Some of the genes (*TNFRSF1A*, *CASP8* and *NFKBIA*) in apoptosis signalling pathways were upregulated by BDE-47 treatment. *TNFRSF1A* belongs to the tumor necrosis factor receptor (*TNFR*) family and its upregulation has been suggested to induce cell death [51]. Upregulation of *CASP8* expression has been linked to execute the apoptotic signaling mainly through extrinsic pathway [52]. Therefore, in view of the apoptotic (subG1) peak in cell cycle, we presume that BDE-47 triggered the apoptosis mediated by *TNFR* family member *via* extrinsic apoptotic pathway. In addition, we also found that *NFKBIA* expression was up regulated, indicating the involvement of *NFKB* pathway. These results suggest that the *NFKB* pathway and related genes could be an important molecular mechanism by which BDE-47 induces apoptosis in HepG2 cells. BDE-47 treated cells showed the down regulation of *CYP1A1* and *CYP2E1* genes. The cytochrome 450s (*CYP450s*) protein superfamily is mainly involved in the oxidation of endogenous, as well as exogenous chemical substrates. *CYP1A1* and *CYP2E1* are among the prominent nine isoforms of *CYP450s*, which are capable of metabolizing majority of drugs or toxins in humans [53]. We found that *IL1b*, *IL-6*, *TNF* and *NFKB1* genes were down regulated in the treated cells, which may be attributed to the anti-inflammatory potential of BDE-47. The down regulation of *CYP1A1* and *CYP2E1* is linked with the inflammatory genes, as it is reported that *IL-6* suppresses the levels of the mRNAs for *CYP1A1* in human hepatoma cell lines [54]. On the other hand, *IL1* reported to inhibit *CYP1A1* expression in hepatocytes [55]. The under expression of *IL1b* and *IL-6* is also regulated through the suppression of *NFKB* and *MAPK* pathways [56,57]. Nonetheless, *TNF* plays an important role in immune cells regulation, and its dysregulation has been implicated in a variety of inflammatory diseases. Therefore, the immune mediators are capable of downregulating *CYP450s* gene expressions, and that some of these effects may be specific for certain P450 isozymes or groups of isozymes [58].

Oxidative stress has been considered as a critical reason for the expressional regulation of *CYP450s* isoforms [59]. In this context, the upregulation of oxidative and metabolic stress genes *viz*. *HMOX1*, *SOD2*, *PRDX1* and *PTGS1* by BDE-47 suggests the activa-

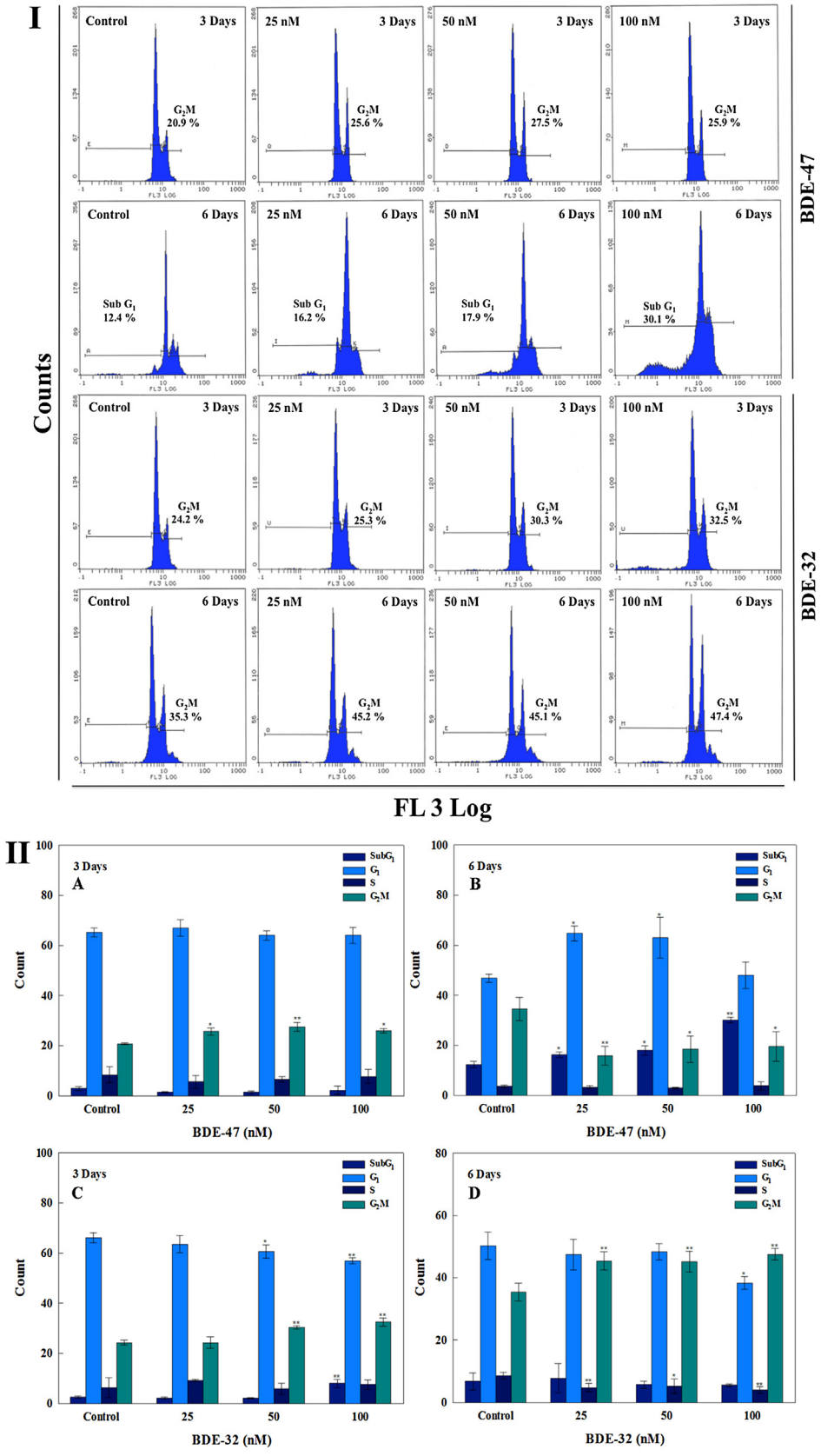

Fig. 5. Flow cytometric images in panel I showing the dysregulation of normal cell cycle in HepG2 cells after BDE-47 and BDE-32 treatments. Panel II shows the average values expressed as population of cells in subG$_1$, G$_1$, S and G$_2$/M phases of cell cycle after BDE-47 (A and B) and BDE-32 (C and D) treatments. $^{*}p < 0.05$, $^{**}p < 0.01$ *versus* control.

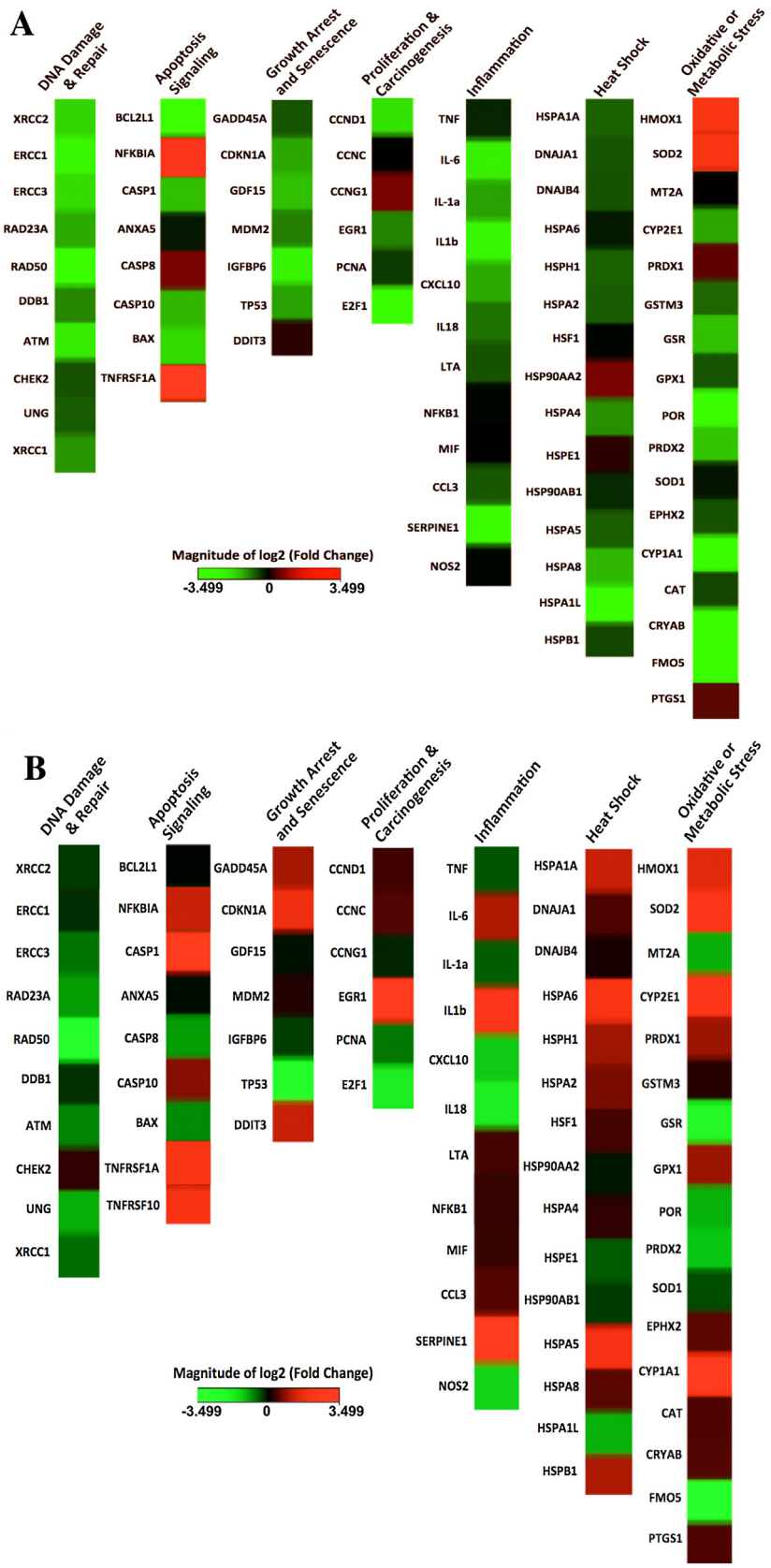

Fig. 6. qPCR array of oxidative stress and toxicity pathway genes in HepG2 cells. Heat map showing the relative gene expression of 84 genes responsible for human stress and toxicity pathway in (A) BDE-47 (100 nM) and (B) BDE-32 (100 nM) treated HepG2 cells after 6 days of exposure.

tion of protective mechanism to overcome the oxidative stress. However, under the influence of severe toxicity of BDE-47, HepG2 antioxidant protective mechanisms were compromised and cells became apoptotic, which is clearly evident by our flow cytometric data. Consequently, the oxidative stress and failure of anti-oxidant protective mechanism unequivocally suggests the role of ROS in downregulating *CYP1A1* and *CYP2E1* expressions in BDE-47 treated cells. Oxidative stress in general has been implicated for the inhibition of *CYP1A1* RNA expression, which could be a factor for transcriptional repression of *CYP1A1* gene [60]. In a recent study, the aryl hydrocarbon receptor (*AhR*) gene expression was altered in larvae of zebrafish treated with BDE-47 [61]. This interpretation is in line with the role of ROS in disrupting aryl hydrocarbon receptor (*AhR*)-dependent expression of *CYP1A1*, which represents a protective negative feedback loop [62]. Hence, we also suspect the putative role of ROS in damaging *AhR* of HepG2 cells in deregulating the expression *CYPP450* isoforms.

On the other hand, BDE-32 treatment resulted in the upregulation of *EGR1*, *MDM2*, *GADD45A* and *DDIT3* genes in HepG2 cells. Induction of an early response gene (*EGR1*) may be directly related to oxidative stress *per se*, it is rapidly induced by a broad spectrum of factors *viz.* environmental stress, DNA repair, DNA damage, mitochondria and cell membrane impairment [63–66]. Therefore, BDE-32 induced mitochondrial dysfunction, DNA damage and ROS formation validate the overexpression of *EGR1* in HepG2 cells. Also, the *EGR1* overexpression resembles previous finding demonstrating mitochondrial dysfunction in hepatoma cells treated with the anti-HIV drug [67]. BDE-32 increased the expression of *DDIT3* and *GADD45A* transcripts, which can be correlated with the properties of *EGR1* to initiate *DDIT3* and *GADD45* family genes by binding to 5′-flanking regions, especially under stressed conditions [68–70]. BDE-32 exposure resulted in downregulation of *TP53*, one reason for this downregulation could be the activation of *NFKB1*. It is known that *NFKB* can suppress *P53* levels by up regulating *MDM2* expression mediated through B-cell CLL/lymphoma 3 (Bcl3) [71]. As oxidative stress increases, cellular response progresses from the activation of antioxidant defense to inflammation and eventually cell death [72,73]. The oxidative stress induced by BDE-32 is also evidenced by an increase in the expression of *HMOX1* and *SOD2* genes. Activation of these genes represent a protective response in rescuing the cells from cell death, which is clearly evident by the absence of subG1 apoptotic peaks in our flow analysis. Our data is in accordance with a recent report on human bronchial epithelial cells exposed to organic extract of particulate matter emissions, showing an elevated expression of *HMOX1* and *SOD2* genes [74]. We found that BDE-32 upregulated the inflammatory cytokines (*IL-6*, *IL1b*, *NFKB1*), suggesting its pro-inflammatory potential. These observations are in line with the activation of *IL-6*, *IL1b*, *CYP1A1* and *NFKB* genes in human bronchial epithelial cells exposed to diesel engine exhaust particles [75]. *IL-6* is a well known responder to cellular injury, and helps to regulate the acute phase inflammatory response [76,77]. Nevertheless, a cross talk between *CYP1A1* upregulation and activated pro-inflammatory cytokines has been described previously [78]. *CYP1A1* is known to induce by the *AhR*-pathway, and its protein plays an essential function in the biotransformation and detoxification of endogenous and exogenous compounds [79]. Similarly, *CYP2E1* has also been reported to actively involve in the oxidative metabolic processing of xenobiotics, drugs, steroid hormones and triglycerides [80]. Hence, the activation of *CYP1A1* and *CYP2E1* genes suggests an enhanced metabolism of BDE-32 in exposed cells. We presume that the upregulation of *CYP1A1*, *CYP2E1* and inflammatory cytokines may have been mediated by the *AhR*, which is reported to upregulate the expression *IL-1b* and *IL-6* genes [81,82]. Since BDE-32 lacks proper scientific attention, the mechanism of *AhR*-based activation of *CYP450s* isoforms would be an important aspect of future research. Moreover, BDE-32 exposure resulted in the upregulation of *CDKN1A* gene. Under the stressed condition, upregulation of *CDKN1A* and *IL-6* genes have been linked to induce cell cycle arrest, cell proliferation and growth arrest [83,84]. Therefore, upregulation of both genes (*CDKN1A* and *IL-6*) corroborate well with BDE-32 induced G_2/M arrest in HepG2 cells after 3 and 6 days.

5. Conclusions

The present study demonstrates that BDE-47 has induced heavy oxidative stress, DNA damage and alters the mitochondrial membrane function in HepG2 cells. These cellular anomalies were beyond the repair capacity, thus apoptotic events were triggered in HepG2 cells. An overall down regulation of genes in PCR array suggested pleiotropic effect of BDE-47 to induced cell death. The downregulation of inflammatory genes (*IL1b*, *IL-6*, *TNF* and *NFKB1*) suggested the anti-inflammatory nature of BDE-47, which may be linked with the downregulation of *CYP450s* isoforms in this study. The downregulation of both *CYP450s* isoforms (*CYP1A1* and *CYP2E1*) indicate the possible role of BDE-47 to damage HepG2-*AhR* regulatory mechanism.

This first report on BDE-32 provide novel information on the cellular toxicity and DNA damage, which may be attributed to the excessive intracellular ROS generation and dysfunction of $\Delta\Psi m$ in HepG2 cells. Interestingly, we found cell cycle (G_2/M) arrest in cells, suggesting the vitality of repair system to rectify the DNA damage. In order to preclude the apoptotic cell death, upregulation of *EGR1*, *MDM2*, *GADD45A*, *DDIT3*, *HMOX1* and *SOD2* genes plays an important role in the BDE-32 treated cells. While, the upregulation of *CYP1A1*, *CYP2E1* and inflammatory cytokines (*IL-6*, *IL1b* and *NFKB1*) suggests the possible role of *AhR* mediated biotransformation of BDE-32. Nonetheless, the over and under expression of genes related to different cellular pathways suggested the likely hood of cellular anomalies including impaired nucleotide excision repair, homologous recombination or base excision repair by both congeners. However, all these expressional analyses deserve further investigations on the translational activation of proteins and related biological meanings.

Conflict of interest

The authors declare no conflict of interest.

Acknowledgements

This project was funded by the National Plan for Science, Technology and Innovation (MAARIFAH), King Abdul Aziz City for Science and Technology, Kingdom of Saudi Arabia, Award Number 13-ENV2116-02.

Appendix A. Supplementary data

Supplementary data associated with this article can be found, in the online version, at http://dx.doi.org/10.1016/j.jhazmat.2016.01.025.

References

[1] M. Frederiksen, K. Vorkamp, M. Thomsen, L.E. Knudsen, Human internal and external exposure to PBDEs—a review of levels and sources, Int. J. Hyg. Environ. Health 212 (2009) 109–134, http://dx.doi.org/10.1016/j.ijheh.2008.04.005.

[2] A. Sjödin, D.G. Patterson Jr., A. Bergman, A review on human exposure to brominated flame retardants-particularly polybrominated diphenyl ethers, Environ. Int. 29 (2003) 829–839, http://dx.doi.org/10.1016/S0160-4120(03)00108-9.

[3] A. Bradman, R. Castorina, F. Gaspar, M. Nishioka, M. Colón, W. Weathers, P.P. Egeghy, R. Maddalena, J. Williams, P.L. Jenkins, T.E. McKone, Flame retardant

exposures in California early childhood education environments, Chemosphere 116 (2014) 61–66, http://dx.doi.org/10.1016/j.chemosphere.2014.02.072.
[4] S. Harrad, C.A. de Wit, M.A. Abdallah, C. Bergh, J.A. Björklund, A. Covaci, P.O. Darnerud, J. de Boer, M. Diamond, S. Huber, P. Leonards, M. Mandalakis, C. Ostman, L.S. Haug, C. Thomsen, T.F. Webster, Indoor contamination with hexabromocyclododecanes, polybrominated diphenyl ethers, and perfluoroalkyl compounds: an important exposure pathway for people? Environ. Sci. Technol. 44 (2010) 3221–3231, http://dx.doi.org/10.1021/es903476t.
[5] J.A. Nanes, Y. Xia, R.M. Dassanayake, R.M. Jones, A. Li, C.J. Stodgell, C.K. Walker, S. Szabo, S. Leuthner, M.S. Durkin, J. Moye, R.K. Miller, Selected persistent organic pollutants in human placental tissue from the United States, Chemosphere 106 (2014) 20–27, http://dx.doi.org/10.1016/j.chemosphere.2013.12.080.
[6] G. Choi, S. Kim, S. Kim, S. Kim, Y. Choi, H.J. Kim, J.J. Lee, S.Y. Kim, S. Lee, H.B. Moon, S. Choi, K. Choi, J. Park, Occurrences of major polybrominated diphenyl ethers (PBDEs) in maternal and fetal cord blood sera in Korea, Sci. Total Environ. 491–492 (2014) 219–226, http://dx.doi.org/10.1016/j.scitotenv.2014.02.071.
[7] F. Huang, S. Wen, J. Li, Y. Zhong, Y. Zhao, Y. Wu, The human body burden of polybrominated diphenyl ethers and their relationships with thyroid hormones in the general population in Northern China, Sci. Total Environ. 466–467 (2014) 609–615, http://dx.doi.org/10.1016/j.scitotenv.2013.07.008.
[8] C.A. de Wit, An overview of brominated flame-retardants in the environment, Chemosphere 46 (2002) 583–624, http://dx.doi.org/10.1016/S0045-6535(01)00225-9.
[9] J.B. Herbstman, A. Sjödin, M. Kurzon, S.A. Lederman, R.S. Jones, V. Rauh, L.L. Needham, D. Tang, M. Niedzwiecki, R.Y. Wang, F. Perera, Prenatal exposure to PBDEs and neurodevelopment, Environ. Health Perspect. 118 (2010) 712–719, http://dx.doi.org/10.1289/ehp.0901340.
[10] M. Wahl, B. Lahni, R. Guenther, B. Kuch, L. Yang, U. Straehle, S. Strack, C. Weiss, A technical mixture of 2,2′,4,4′-tetrabromo diphenyl ether (BDE47) and brominated furans triggers aryl hydrocarbon receptor (AhR) mediated gene expression and toxicity, Chemosphere 73 (2008) 209–215, http://dx.doi.org/10.1016/j.chemosphere.2008.05.025.
[11] T. Yan, L. Xiang, J. Xuejun, C. Chengzhi, Q. Youbin, Y. Xuelan, L. Yang, P. Changyan, C. Hui, Spatial learning and memory deficit of low level polybrominated diphenyl ethers-47 in male adult rat is modulated by intracellular glutamate receptors, J. Toxicol. Sci. 37 (2012) 223–233, http://dx.doi.org/10.2131/jts.37.223.
[12] Z. Zhang, X. Zhang, Z. Sun, H. Dong, L. Qiu, J. Gu, J. Zhou, X. Wang, S.L. Wang, Cytochrome P450 3A1 mediates 2,2′,4,4′-tetrabromodiphenyl ether induced reduction of spermatogenesis in adult rats, PLoS One 8 (6) (2013) e66301, http://dx.doi.org/10.1371/journal.pone.0066301.
[13] J.S. Kim, J. Klösener, S. Flor, T.M. Peters, G. Ludewig, P.S. Thorne, L.W. Robertson, G. Luthe, Toxicity assessment of air-delivered particle-bound polybrominated diphenyl ethers, Toxicology 317 (2014) 31–39, http://dx.doi.org/10.1016/j.tox.2014.01.005.
[14] C. Yan, D. Huang, Y. Zhang, The involvement of ROS overproduction and mitochondrial dysfunction in PBDE-47-induced apoptosis on Jurkat cells, Exp. Toxicol. Pathol. 63 (2011) 413–417, http://dx.doi.org/10.1016/j.etp.2010.02.018.
[15] S.C. Huang, G. Giordano, L.G. Costa, Comparative cytotoxicity and intracellular accumulation of five polybrominated diphenyl ether congeners in mouse cerebellar granule neurons, Toxicol. Sci. 114 (2010) 124–132, http://dx.doi.org/10.1093/toxsci/kfp296.
[16] H.R. Park, P.W. Kamau, R. Loch-Caruso, Involvement of reactive oxygen species in brominated diphenyl ether-47-induced inflammatory cytokine release from human extravillous trophoblasts in vitro, Toxicol. Appl. Pharmacol. 274 (2014) 283–292, http://dx.doi.org/10.1016/j.taap.2013.11.015.
[17] P. He, A.G. Wang, T. Xia, P. Gao, Q. Niu, L.J. Guo, B.Y. Xu, X.M. Chen, Mechanism of the neurotoxic effect of PBDE-47 and interaction of PBDE-47 and PCB153 in enhancing toxicity in SH-SY5Y cells, Neurotoxicology 30 (2009) 10–15.
[18] S. Zhang, G. Kuang, G. Zhao, X. Wu, C. Zhang, R. Lei, T. Xia, J. Chen, Z. Wang, R. Ma, B. Li, L. Yang, A. Wang, Involvement of the mitochondrial p53 pathway in PBDE-47-induced SH-SY5Y cells apoptosis and its underlying activation mechanism, Food Chem. Toxicol. 62 (2013) 699–706, http://dx.doi.org/10.1016/j.fct.2013.10.008.
[19] S. Tagliaferri, A. Caglieri, M. Goldoni, S. Pinelli, R. Alinovi, D. Poli, C. Pellacani, G. Giordano, A. Mutti, L.G. Costa, Low concentrations of the brominated flame retardants BDE-47 and BDE-99 induce synergistic oxidative stress-mediated neurotoxicity in human neuroblastoma cells, Toxicol. In Vitro 24 (2010) 116–122, http://dx.doi.org/10.1016/j.tiv.2009.08.020.
[20] X. Liu, J. Wang, C. Lu, C. Zhu, B. Qian, Z. Li, C. Liu, J. Shao, J. Yan, The role of lysosomes in BDE 47-mediated activation of mitochondrial apoptotic pathway in HepG2 cells, Chemosphere 124 (2015) 10–21, http://dx.doi.org/10.1016/j.chemosphere.2014.10.054.
[21] L.S. Birnbaum, Applying research to public health questions: timing and environmentally relevant dose, Environ. Health Perspect. 117 (2009) A478, http://dx.doi.org/10.1289/ehp.0901417.
[22] R.G. Wei, Y.X. Zhao, P.Y. Liu, Z.F. Qin, S.S. Yan, Y. Li, X.F. Qin, X.J. Xia, X.B. Xu, M.C. Yan, Determination of environmentally relevant exposure concentrations of polybrominated diphenyl ethers for in vitro toxicological studies, Toxicol. In Vitro 24 (2010) 1078–1085, http://dx.doi.org/10.1016/j.tiv.2010.03.015.
[23] L. Wang, W. Zou, Y. Zhong, J. An, X. Zhang, M. Wu, Z. Yu, The hormesis effect of BDE-47 in HepG2 cells and the potential molecular mechanism, Toxicol. Lett. 209 (2012) 193–201, http://dx.doi.org/10.1016/j.toxlet.2011.12.014.
[24] H. Wang, H. Cheng, F. Wang, D. Wei, X. Wang, An improved 3-(4,5-dimethylthiazol-2-yl)-2,5-diphenyl tetrazolium bromide (MTT) reduction assay for evaluating the viability of *Escherichia coli* cells, J. Microbiol. Methods 82 (2010) 330–333, http://dx.doi.org/10.1016/j.mimet.2010.06.014.
[25] Q. Saquib, A.A. Al-Khedhairy, J. Ahmad, M.A. Siddiqui, S. Dwivedi, S.T. Khan, J. Musarrat, Zinc ferrite nanoparticles activate IL-1b, NFKB1, CCL21 and NOS2 signaling to induce mitochondrial dependent intrinsic apoptotic pathway in WISH cells, Toxicol. Appl. Pharmacol. 273 (2013) 289–297, http://dx.doi.org/10.1016/j.taap.2013.09.001.
[26] G. Repetto, A. del Peso, J.L. Zurita, Neutral red uptake assay for the estimation of cell viability/cytotoxicity, Nat. Protoc. 3 (2008) 1125–1131, http://dx.doi.org/10.1038/nprot.2008.75.
[27] O. Myhre, J.M. Andersen, H. Aarnes, F. Fonnum, Evaluation of the probes 2′, 7′-dichlorofluorescin diacetate, luminol, and lucigenin as indicators of reactive species formation, Biochem. Pharmacol. 65 (2003) 1575–1582, http://dx.doi.org/10.1016/S0006-2952(03)00083-2.
[28] Q. Saquib, J. Musarrat, M.A. Siddiqui, S. Dutta, S. Dasgupta, J.P. Giesy, A.A. Al-Khedhairy, Cytotoxic and necrotic responses in human amniotic epithelial (WISH) cells exposed to organophosphate insecticide phorate, Mutat. Res. 744 (2012) 125–134, http://dx.doi.org/10.1016/j.mrgentox.2012.01.001.
[29] Q. Saquib, A.A. Al-Khedhairy, M.A. Siddiqui, F.M. Abou-Tarboush, A. Azam, J. Musarrat, Titanium dioxide nanoparticles induced cytotoxicity, oxidative stress and DNA damage in human amnion epithelial (WISH) cells, Toxicol. In Vitro 26 (2012) 351–361, http://dx.doi.org/10.1016/j.tiv.2011.12.011.
[30] Q. Saquib, A.A. Al-Khedhairy, S. Al-Arifi, A. Dhawan, J. Musarrat, Assessment of methyl thiophanate-Cu(II) induced DNA damage in human lymphocytes, Toxicol. In Vitro 23 (2009) 848–854, http://dx.doi.org/10.1016/j.tiv.2009.04.017.
[31] R.A. Hites, Polybrominated diphenyl ethers in the environment and in people: a meta-analysis of concentrations, Environ. Sci. Technol. 38 (2004) 945–956, http://dx.doi.org/10.1021/es035082g.
[32] A. Sjödin, L.Y. Wong, R.S. Jones, A. Park, Y. Zhang, C. Hodge, E. Dipietro, C. McClure, W. Turner, L.L. Needham, D.G. Patterson Jr., Serum concentrations of polybrominated diphenyl ethers (PBDEs) and polybrominated biphenyl (PBB) in the United States population, Environ. Sci. Technol. 42 (2008) 1377–1384, http://dx.doi.org/10.1021/es702451p.
[33] W. He, P. He, A. Wang, T. Xia, B. Xu, X. Chen, Effects of PBDE-47 on cytotoxicity and genotoxicity in human neuroblastoma cells in vitro, Mutat. Res. 649 (2008) 62–70, http://dx.doi.org/10.1016/j.mrgentox.2007.08.001.
[34] M. Zhao, F. Antunes, J.W. Eaton, U.T. Brunk, Lysosomal enzymes promote mitochondrial oxidant production, cytochrome c release and apoptosis, Eur. J. Biochem. 270 (2003) 3778–3786, http://dx.doi.org/10.1046/j. 1432-1033.2003.03765.x.
[35] A. Baracca, G. Sgarbi, G. Solaini, G. Lenaz, Rhodamine 123 as a probe of mitochondrial membrane potential: evaluation of proton flux through F(0) during ATP synthesis, Biochim. Biophys. Acta 1606 (2003) 137–146, http://dx.doi.org/10.1016/S0005-2728(03)00110-5.
[36] J. Shao, C.C. White, M.J. Dabrowski, T.J. Kavanagh, M.L. Eckert, E.P. Gallagher, The role of mitochondrial and oxidative injury in BDE 47 toxicity to human fetal liver hematopoietic stem cells, Toxicol. Sci. 101 (2008) 81–90, http://dx.doi.org/10.1093/toxsci/kfm256.
[37] A. Lejay, A. Meyer, A.I. Schlagowski, A.L. Charles, F. Singh, J. Bouitbir, J. Pottecher, N. Chakfe, J. Zoll, B. Geny, Mitochondria: mitochondrial participation in ischemia-reperfusion injury in skeletal muscle, Int. J. Biochem. Cell Biol. 50 (2014) 101–105, http://dx.doi.org/10.1016/j.biocel.2014.02.013.
[38] M. Crompton, The mitochondrial permeability transition pore and its role in cell death, Biochem. J. 341 (1999) 233–249.
[39] G. Ouédraogo, P. Morlière, R. Santus, M.A. Miranda, J.V. Castell, Damage to mitochondria of cultured human skin fibroblasts photosensitized by fluoroquinolones, Photochem. Photobiol. B 58 (2000) 20–25, http://dx.doi.org/10.1016/S1011-1344(00)00101-9.
[40] P. Haegler, D. Grünig, B. Berger, S. Krähenbühl, J. Bouitbir, Impaired mitochondrial function in HepG2 cells treated with hydroxy-cobalamin[c-lactam]: a cell model for idiosyncratic toxicity, Toxicology 336 (2015) 48–58, http://dx.doi.org/10.1016/j.tox.2015.07.015.
[41] M. Murphy, How mitochondria produce reactive oxygen species, Biochem. J. 417 (2009) 1–13, http://dx.doi.org/10.1042/BJ20081386.
[42] C.G. Ferreira, M. Epping, F.A. Kruyt, G. Giaccone, Apoptosis: target of cancer therapy, Clin. Cancer Res. 8 (2002) 2024–2034.
[43] J. Konopa, G2 block induced by DNA crosslinking agents and its possible consequence, Biochem. Pharmacol. 37 (1988) 2303–2309, http://dx.doi.org/10.1016/0006-2952(88)90355-3.
[44] Y.P. Tsao, P. D'Arpa, L.F. Liu, The involvement of active DNA synthesis in camptothecin-induced G2 arrest: altered regulation of p34cdc2/cyclin B, Cancer Res. 52 (1992) 1823–1829.
[45] M.M. Manson, B.E. Foreman, L.M. Howells, E.P. Moiseeva, Determining the efficacy of dietary phytochemicals in cancer prevention, Biochem. Soc. Trans. 35 (2007) 1358–1363, http://dx.doi.org/10.1042/BST0351358.
[46] L.J. Niedernhofer, H. Odijk, M. Budzowska, E. van Drunen, A. Maas, A.F. Theil, J. de Wit, N.G. Jaspers, H.B. Beverloo, J.H. Hoeijmakers, R. Kanaar, The structure-specific endonuclease Ercc1-Xpf is required to resolve DNA interstrand cross-link-induced double-strand breaks, Mol. Cell. Biol. 24 (2004) 5776–5787, http://dx.doi.org/10.1128/MCB.24.13.5776-5787.2004.

[47] A. Mannuss, O. Trapp, H. Puchta, Gene regulation in response to DNA damage, Biochim. Biophys. Acta 1819 (2012) 154–165, http://dx.doi.org/10.1016/j.bbagrm.2011.08.003.
[48] B.J. You, Y.C. Wu, C.L. Lee, H.Z. Lee, Non-homologous end joining pathway is the major route of protection against 4b-hydroxywithanolide E-induced DNA damage in MCF-7 cells, Food Chem. Toxicol. 65 (2014) 205–212, http://dx.doi.org/10.1016/j.fct.2013.12.026.
[49] E. van Dyk, P.J. Pretorius, Impaired DNA repair and genomic stability in hereditary tyrosinemia type 1, Gene 495 (2012) 56–61, http://dx.doi.org/10.1016/j.gene.2011.12.021.
[50] C. Martins, C. Doran, I.C. Silva, C. Miranda, J. Rueff, A.S. Rodrigues, Myristicin from nutmeg induces apoptosis via the mitochondrial pathway and down regulates genes of the DNA damage response pathways in human leukaemia K562 cells, Chem. Biol. Interact. 218 (2014) 1–9, http://dx.doi.org/10.1016/j.cbi.2014.04.014.
[51] K.F. Chan, M.R. Siegel, J.M. Lenardo, Signaling by the TNF receptor superfamily and T cell homeostasis, Immunity 13 (2000) 419–422, http://dx.doi.org/10.1016/S1074-7613(00)00041-8.
[52] A. Luzio, S.M. Monteiro, A.A. Fontaínhas-Fernandes, O. Pinto-Carnide, M. Matos, A.M. Coimbra, Copper induced upregulation of apoptosis related genes in zebra fish (*Danio rerio*) gill, Aquat. Toxicol. 128–129 (2013) 183–189, http://dx.doi.org/10.1016/j.aquatox.2012.12.018.
[53] W.E. Evans, M.V. Relling, Pharmacogenomics: translating functional genomics into rational therapeutics, Science 286 (1999) 487–491.
[54] Y. Fukuda, N. Ishida, T. Noguchi, A. Kappas, S. Sassa, Interleukin-6 down regulates the expression of transcripts encoding cytochrome P450 IA1: IA2 and IIIA3 in human hepatoma cells Biochem, Biophys. Res. Commun. 184 (1992) 960–965.
[55] C.W. Barker, J.B. Fagan, D.S. Pasco, Interleukin-1β suppresses the induction of P4501A1 and P4501A2 mRNAs in isolated hepatocytes, J. Biol. Chem. 267 (1992) 8050–8055.
[56] H. Zhou, C.S. Beevers, S. Huang, The targets of curcumin, Curr. Drug Targets 12 (2011) 332–347.
[57] J. Epstein, I.R. Sanderson, T.T. Macdonald, Curcumin as a therapeutic agent: the evidence from in vitro animal and human studies, Br. J. Nutr. 103 (2010) 1545–1557.
[58] F. Rusolo, B. Pucci, G. Colonna, F. Capone, E. Guerriero, M.R. Milone, M. Nazzaro, M.G. Volpe, G. Di Bernardo, G. Castello, S. Costantini, Evaluation of selenite effects on selenoproteins and cytokinome in human hepatoma cell lines, Molecules 18 (2013) 254962.
[59] K.M. Kulmatycki, F. Jamali, Drug disease interactions: role of inflammatory mediators in disease and variability in drug response, J. Pharm. Pharm. Sci. 8 (2005) 602–625.
[60] T. Stoeger, S. Takenaka, B. Frankenberger, B. Ritter, E. Karg, K. Maier, H. Schulz, O. Schmid, Deducing in vivo toxicity of combustion-derived nanoparticles from a cell-free oxidative potency assay and metabolic activation of organic compounds, Environ. Health Perspect. 117 (2009) 54–60, http://dx.doi.org/10.1289/ehp.11370.
[61] H. Liu, S. Tang, X. Zheng, Y. Zhu, Z. Ma, C. Liu, M. Hecker, D.M. Saunders, J.P. Giesy, X. Zhang, H. Yu, Bioaccumulation biotransformation, and toxicity of BDE-47, 6-OH-BDE-47, and 6-MeO-BDE-47 in early life-stages of zebrafish (*Danio rerio*), Environ. Sci. Technol. 49 (2015) 1823–1833.
[62] Y. Morel, N. Mermod, R. Barouki, An autoregulatory loop controlling CYP1A1 gene expression: role of H(2)O(2) and NFI, Mol. Cell. Biol. 19 (1999) 6825–6832.
[63] N.A. Franken, R. Ten Cate, C. Van Bree, J. Haveman, Induction of the early response protein EGR-1 in human tumour cells after ionizing radiation is correlated with a reduction of repair of lethal lesions and an increase of repair of sublethal lesions, Int. J. Oncol. 24 (2004) 1027–1031.
[64] G.D. Bothun, Hydrophobic silver nanoparticles trapped in lipid bilayers: size distribution, bilayer phase behavior, and optical properties, J. Nanobiotechnol. 6 (2008) 13, http://dx.doi.org/10.1186/1477-3155-6-13.
[65] W.P. Roos, B. Kaina, DNA damage-induced cell death by apoptosis, Trends Mol. Med. 12 (2006) 440–450, http://dx.doi.org/10.1016/j.molmed.2006.07.007.
[66] J.S. Teodoro, A.M. Simões, F.V. Duarte, A.P. Rolo, R.C. Murdoch, S.M. Hussain, C.M. Palmeira, Assessment of the toxicity of silver nanoparticles in vitro: a mitochondrial perspective, Toxicol. In Vitro 25 (2011) 664–670, http://dx.doi.org/10.1016/j.tiv.2011.01.004.
[67] L.J. Gomez-Sucerquia, A. Blas-Garcia, M. Marti-Cabrera, J.V. Esplugues, N. Apostolova, Profile of stress and toxicity gene expression in human hepatic cells treated with efavirenz, Antiviral Res. 94 (2012) 232–241, http://dx.doi.org/10.1016/j.antiviral.2012.04.003.
[68] J.S. Park, J.D. Luethy, M.G. Wang, J. Fargnoli, A.J. Fornace Jr., O.W. McBride, N.J. Holbrook, Isolation, characterization and chromosomal localization of the human GADD153 gene, Gene 116 (1992) 259–267.
[69] K.C. Manthey, R. Rodriguez-Melendez, J.T. Hoi, J. Zempleni, Riboflavin deficiency causes protein and DNA damage in HepG2 cells, triggering arrest in G1 phase of the cell cycle, J. Nutr. Biochem. 17 (2006) 250–256, http://dx.doi.org/10.1016/j.jnutbio.2005.05.004.
[70] M.B. Frank, Q. Yang, J. Osban, J.T. Azzarello, M.R. Saban, R. Saban, R.A. Ashley, J.C. Welter, K.M. Fung, H.K. Lin, Frankincense oil derived from Boswellia carteri induces tumor cell specific cytotoxicity, BMC Complement. Altern. Med. 9 (2009) 6, http://dx.doi.org/10.1186/1472-6882-9-6.
[71] D. Kashatus, P. Cogswell, A.S. Baldwin, Expression of the Bcl-3 proto-oncogene suppresses p53 activation, Genes Dev. 20 (2006) 225–235, http://dx.doi.org/10.1101/gad.1352206.
[72] N. Li, T. Xia, A.E. Nel, The role of oxidative stress in ambient par-ticulate matter-induced lung diseases and its implications in the toxicity of engineered nanoparticles, Free Radic. Biol. Med. 44 (2008) 1689–1699, http://dx.doi.org/10.1016/j.freeradbiomed.2008.01.028.
[73] A. Nel, T. Xia, L. Madler, N. Li, Toxic potential of materials at the nanolevel, Science 311 (2006) 622–627, http://dx.doi.org/10.1126/science.1114397.
[74] N. Li, P. Bhattacharya, G. Karavalakis, K. Williams, N. Gysel, N. Rivera-Rios, Emissions from commercial-grade charbroiling meat operations induce oxidative stress and inflammatory responses in human bronchial epithelial cells, Toxicol. Rep. 1 (2014) 802–811, http://dx.doi.org/10.1016/j.toxrep.2014.09.015.
[75] A.I. Totlandsdal, F.R. Cassee, P. Schwarze, M. Refsnes, M. Låg, Diesel exhaust particles induce CYP1A1 and pro-inflammatory responses via differential pathways in human bronchial epithelial cells, Part. Fibre Toxicol. 7 (2010) 41, http://dx.doi.org/10.1186/1743-8977-7-41.
[76] M.M. McFarland-Mancini, H.M. Funk, A.M. Paluch, M. Zhou, P.V. Giridhar, C.A. Mercer, S.C. Kozma, A.F. Drew, Differences in wound healing in mice with deficiency of IL-6 versus IL-6 receptor, J. Immunol. 184 (2010) 7219–7228.
[77] M. Kopf, H. Baumann, G. Freer, M. Freudenberg, M. Lamers, T. Kishimoto, R. Zinkernagel, H. Bluethmann, G. Köhler, Impaired immune and acute-phase responses in interleukin-6-deficient mice, Nature 368 (1994) 339–342.
[78] W.A. Pryor, Cigarette smoke radicals and the role of free radicals in chemical carcinogenicity, Environ. Health Perspect. 105 (1997) 875–882.
[79] S. Gui, Z. Zhang, L. Zheng, Y. Cui, X. Liu, N. Li, X. Sang, Q. Sun, G. Gao, Z. Cheng, J. Cheng, L. Wang, M. Tang, F. Hong, Molecular mechanism of kidney injury of mice caused by exposure to titanium dioxide nanoparticles, J. Hazard. Mater. 195 (2011) 365–370, http://dx.doi.org/10.1016/j.jhazmat.2011.08.055.
[80] F.P. Guengerich, Cytochromes P450 drugs, and diseases, Mol. Interv. 3 (2003) 194–204.
[81] Z.W. Lai, C. Hundeiker, E. Gleichmann, C. Esser, Cytokine gene expression during ontogeny in murine thymus on activation of the aryl hydrocarbon receptor by 2,3,7,8-tetrachlorodibenzo-*p*-dioxin, Mol. Pharmacol. 52 (1997) 30–37.
[82] C. Vogel, J. Abel, Effect of 2,3,7,8-tetrachlorodibenzo-*p*-dioxin on growth factor expression in the human breast cancer cell line MCF-7, Arch. Toxicol. 69 (1995) 259–265.
[83] F. Bunz, A. Dutriaux, C. Lengauer, T. Waldman, S. Zhou, J.P. Brown, J.M. Sedivy, K.W. Kinzler, B. Vogelstein, Requirement for p53 and p21 to sustain G2 arrest after DNA damage, Science 282 (1998) 1497–1501, http://dx.doi.org/10.1126/science.282.5393.1497.
[84] D.C. Sanford, J.W. DeWille, C/EBPdelta is a downstream mediator of IL-6 induced growth inhibition of prostate cancer cells, Prostate 63 (2005) 143–154, http://dx.doi.org/10.1002/pros.20159.